https://doi.org/10.5194/egusphere-2026-4597
Preprint. Discussion started: 15 September 2026

Comparative Study of HEC-RAS and TELEMAC for Two-Dimensional Flood Simulation in a Densely Built Urban Area

Ardy Nur Ahmadito [1], Leon Frederik De Vos [2], Faizal Immaddudin Wira Rohmat [3], Muhammad Syahril Badri Kusuma [3]

[1] Master Program of Water Resources Management, Institut Teknologi Bandung, Jalan Ganesa No. 10, Bandung 40132, West Java, Indonesia
[2] Chair of Hydraulic Engineering, Technical University of Munich, 80333 Munich, Germany
[3] Water Resources Engineering Research Group, Faculty of Civil and Environmental Engineering, Institut Teknologi Bandung, Jalan Ganesa No. 10, Bandung 40132, West Java, Indonesia

Correspondence to: Faizal I. W. Rohmat (faizalrohmat@itb.ac.id)

Abstract. Flooding is a natural disaster and a long-term challenge for urban planning. Numerous studies have stated how flood risk could increase with climate change and urbanization. HEC-RAS and TELEMAC are some of the sophisticated two-dimensional modelling tools to simulate floods. However, they have different numerical schemes, especially their meshing and discretization. A comparison is needed to evaluate how their results can differ. This study simulated a historical flood event in Sapan, a region in the Upper Citarum Watershed, Indonesia, using HEC-RAS and TELEMAC. Additionally, this study investigated how both models simulate flood extent, propagation, velocities, and depths, especially from TELEMAC since it is underutilized in Indonesia. The models' setup was configured to be equivalent. However, differences remain, especially in the building interpretation. The flood extent from both models was remarkably similar, with a 1.34% difference in max inundated area. The main differences were velocity distribution around buildings because TELEMAC had a finer mesh. However, with a coarser mesh, HEC-RAS could simulate a similar flood extent through the utilization of subgrid bathymetry information. Both models have demonstrated good performance. HEC-RAS might be more suitable for broad-scale modelling, where inundation depth is the main concern. However, if detailed velocity mapping is needed, TELEMAC might be more suitable.

Short summary: This study compares building-integrated flood simulations with HEC-RAS and TELEMAC. Both models demonstrated adequate performance, but major discrepancies were observed, which were mainly driven by different mesh architectures. The findings highlight each model's advantages and disadvantages as well as its potential best usage and recommended adequate model setups for an optimal result.

1 Introduction

Flooding is among the most frequent disasters worldwide, affecting the economy as well as society at large (Khatooni et al., 2025). It constitutes the most prevalent natural disaster globally, accounting for more than 50% of all recorded disasters

https://doi.org/10.5194/egusphere-2026-4597
Preprint. Discussion started: 15 September 2026

between 1990 and 2020 (Avila-Aceves et al., 2023). Although flooding has occurred throughout human history (Angelakis et al., 2023), its severity is increasing in light of land-cover change, population growth, and the increasing climate change effects (Cea & Costabile, 2022; Enu et al., 2025). The interaction between elevated hazard levels and growing socioeconomic vulnerability has made flooding a critical challenge for sustainable development and public safety worldwide (C. Li et al., 2022). Understanding flood risk has become increasingly important, as effective mitigation requires not only quantifying the physical characteristics of flood hazards but also evaluating their potential impacts on exposed communities, infrastructure, and economic activities (Winsemius et al., 2016).

Flood risk itself is commonly defined as a combination of flood hazard, exposure, and the capacity of a community to cope with flood events. In terms of quantifying flood hazard, inundation depth alone cannot fully characterize the severity of a flood (Isma et al., 2024). Flow velocity plays an equally important role in determining structural damage, debris transport, and eventually human safety risks (Adeke & Mugume, 2025). Recent studies have incorporated velocity into urban flood damage assessment, including in the aspects of building vulnerability to flood flows (Luo et al., 2020; Milanesi et al., 2018), human stability in floodwaters (Ribeiro et al., 2021), as well as human entrapment (Cheng et al., 2026). These studies highlight the importance of hydraulic models that are capable of accurately modeling not only flood inundation extent and depth, but also the spatial distribution of flood velocity.

Two-dimensional hydrodynamic models are becoming increasingly important for simulating flood depth and velocity in urban flood hazard assessment. Many software modeling tools are available, each employing different numerical approaches and spatial discretization schemes. Among the widely used are HEC-RAS and TELEMAC. HEC-RAS for example, has been used to evaluate flood hazards and risk assessment in urban areas (Al-Hussein et al., 2026; Feng et al., 2024; García Martínez et al., 2025), used for machine learning (Bhattarai et al., 2024), and coupled to other software such as SWMM (Khatooni et al., 2025). It utilizes a finite-volume method with sub-grid bathymetry. The approach allows for terrain variations inside each cell to distribute flood volume without requiring extremely fine meshes and thus a lot of computational effort (USACE Hydrologic Engineering Center, 2024); however, if there is any sharp topography or structure involved in the domain, a coarse mesh may not simulate flood velocity and momentum correctly. In contrast, TELEMAC utilizes the finite-element method at its core, which requires finer meshes to calculate over complex bathymetry and hydraulic structures accurately. As an example, it has also been implemented for general flood risk assessment and mitigation strategies (De Vos, Mahajan, Caviedes-Voullième, & Rüther, 2026; Houngue et al., 2023; Vu et al., 2015) and application of nature-based solutions (Enu et al., 2025), as well as coupled to SWMM (Wang et al., 2024).

HEC-RAS is more widely used in Indonesia due to its accessibility and large user community, e.g., in the Majalaya flood case (Rohmat et al., 2022), Citeureup (Farid et al., 2026), Makassar (Wulandari et al., 2025), and Nusantara Capital City (Handyastono et al., 2025). On the other hand, TELEMAC has limited but growing application (Abusyarif et al., 2023). Although it would typically require a very fine mesh and a high computational cost, the finer spatial resolution may provide a more accurate representation of velocity fields. Such differences may become relevant for flood risk studies that require velocity as a central assessment variable, e.g., flood flow in an area with densely populated buildings. Despite the software's

https://doi.org/10.5194/egusphere-2026-4597
Preprint. Discussion started: 15 September 2026

widespread use, direct comparisons between HEC-RAS and TELEMAC are limited. It is difficult to determine whether differences in the model originate in terrain discretization, mesh architecture, numerical formulation, or building representation, especially when the two compared models are under non-equivalent configurations (Kesserwani, 2013).

In this study, we aim to develop equivalent HEC-RAS and TELEMAC models for a historical flood event in Sapan, Indonesia. The objectives of this study are to (i) quantify differences in predicted inundation extent, flood propagation, water depth, and flow velocity; (ii) identify the extent to which these differences arise from numerical formulation and building representation; and (iii) discuss the practical implications of model selection for different urban flood modeling applications. We aim to compare and quantify flood modeling result characteristics with identical terrain, hydraulic parameters, and boundary conditions. The differences in mesh architecture, numerical formulation, and building representation inherent to each model were preserved.

2 Materials and Methods

2.1 Study Area

Indonesia experiences frequent floods, with regional annual rainfall up to 4500 mm and is projected to have shifting rainfall patterns, such as higher intensity and frequency of extreme occurrence (Aminah et al., 2024; Kardhana et al., 2024; Rohmat et al., 2023). Floods occur across the archipelago, with more than one thousand flood events recorded annually from 2021 to 2025 (Badan Nasional Penanggulangan Bencana, 2026). Among the many flood-prone areas, the Citarum River in West Java Province experiences some of the most persistent flooding due to intense rainfall, rapid urbanization, and extensive land cover change (Oktaviani et al., 2021). The Citarum River Basin (6830 km2 area) is one of the most important river basins in Indonesia, supplying water to more than 25 million people (including the capital city of Jakarta), supplying water to three large cascade dams, irrigating more than 200,000 ha of paddy fields, hydropower, and many other purposes (Kardhana et al., 2024; Prawirakusuma, 2023; Rohmat et al., 2022). The Citarum River originates from the headwaters in Cisanti Lake and ends at the estuary to the Java Sea. Besides its importance, Citarum has many flood hotspots, including Majalaya, Sapan, and Dayeuhkolot (Kardhana et al., 2024; Rohmat et al., 2022).

The Sapan area is particularly interesting for its location at the confluence of three large tributaries of the Citarum River: the Citarum headstream, Citarik tributary, and Cikeruh tributary (Fig. 1). The confluence of the Citarum headstream tributaries, combined with the low-gradient natural floodplain of the Upper Citarum Watershed, creates backwater effects and flow interactions that make the area prone to flooding (Syuhada et al., 2023). Cheaper land prices compared to city centers caused urban sprawl next to industrial areas, despite the predominant alluvial fan soil and lack of clean water and other public services, demonstrating a lack of effective planning institutions (Nurrokhman et al., 2026). The flood vulnerability is aggravated by the relative ground elevation of the vast floodplains that are only a few meters higher than the typical river's water stage. Only few limited parts of the Sapan area have levees, which leaves many residents directly exposed to flood hazards. Bridges in the area require a high deck rising a couple of meters above the road to ensure sufficient freeboard.

https://doi.org/10.5194/egusphere-2026-4597
Preprint. Discussion started: 15 September 2026

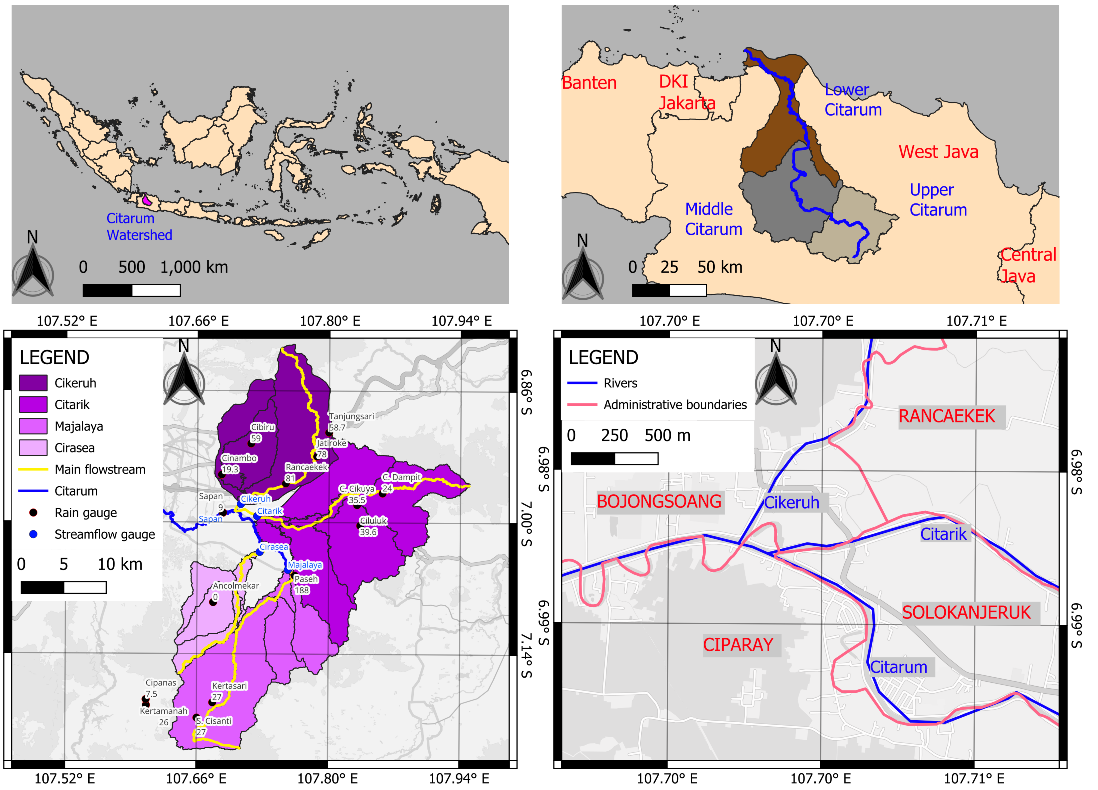

Figure 1: (a) Citarum Watershed relative to Indonesia, (b) the Upper Citarum Watershed relative to Citarum Watershed where the Sapan area is located, (c) all watersheds flowing into Sapan area as well as the observed daily rainfall in mm at each rain gauge on 23rd February 2018, and (d) the detailed Sapan confluence system. Base map data provided by ©OpenStreetMap contributors, via VersaTiles.

2.2 Input Data

This study uses a historical flood from the 23rd of February 2018 as the reference event. Although there are no recorded flood extents, local community social media indicates inundation depth of an adult knee's height (sekitarbandungcom, 2018), which might not be the most extreme magnitude, but is still a flood with considerable hazard potential. Hydrological analysis used terrain data from Indonesia's 8x8 resolution DEMNAS (Digital Elevation Model Nasional) and RBI (Rupa Bumi Indonesia), publicly accessible from tanahairindonesia.go.id (Badan Informasi Geospasial, 2018, 2019). Land cover was obtained from Indonesia's Ministry of Environment and Forestry (KLHK) while soil type was from NASA's HSG database (Ross et al., 2018). The rainfall gauge and Automatic Water Level Recorder (AWLR) shown in Fig. 1 (c) provide detailed reading every 10 minutes but is only available since 2025 and was used for hydrological model calibration. The only available long-term dataset was a daily rainfall observation from 2001 to 2023, which was used to estimate flood discharge. Cikeruh and Citarik have an AWLR station near their outlet, while Citarum has its measurement gauge further upstream at Majalaya Gauge and in

https://doi.org/10.5194/egusphere-2026-4597
Preprint. Discussion started: 15 September 2026

one of its tributaries, Cirasea Gauge. For hydraulic modelling purposes, a detailed 2x2 resolution LiDAR generated Digital Terrain Model (DTM) obtained from Indonesia's Geospatial Information Agency (BIG) and river bathymetry data from Citarum River Basin Organization (BBWS Citarum) were used. Building outline is obtained from OpenStreetMap (2025).

Table 1: Overview of types, sources, timeframes, and specifications of the data utilized for hydrological analysis and hydraulic modelling.

Type	Data	Source	Year	Specification
Rainfall Data	Daily rainfall	BMKG, BBWS Citarum	2001-2023	mm/day
	10-min interval observation	KOICA-BBWS Citarum	2025	mm
Observed Flow	10-min interval observation	KOICA-BBWS Citarum	2025	m^3/s
Topography (Watershed Terrain)	DEMNAS	BIG	2018	DEM 8x8 m
	RBI	BIG	2019	Contour map
Topography (Hydraulic Model Terrain)	Floodplain LiDAR	BIG	2025	DTM 2x2 m
	River bathymetry	BBWS Citarum	2023	DEM 0.5x0.5 m
Buildings	Building outline	OpenStreetMap	2025	Vector polygons
Land cover	Official Indonesian Land Cover Shapefiles	KLHK	2019	30x30 m
Soil type	Hydrologic Soil Group	NASA	2018	250x250 m

2.3 Research Framework

Flowchart for this study is shown in Fig. 2. It consists of five main phases: watershed delineation, rainfall preprocessing, hydrological model, hydraulic model, and subsequently, comparative analysis.

2.3.1 Watershed Delineation and Rainfall Preprocessing

The study started with delineating watershed system that flows to the study area, the result of which is shown in Fig. 1. It was done with a combination of manual contour-based delineation and HEC-HMS delineation tool with terrain reconditioning. Due to limited discharge observation, a recorded daily rainfall data at the day of the flood event was obtained from the long-term dataset and was used to generate a synthetic hydrograph. The detailed 10-min interval rain and streamflow observations were utilized to calibrate the hydrological model. Rainfall data was averaged over each watershed area using Voronoi polygon-based area averaging.

https://doi.org/10.5194/egusphere-2026-4597
Preprint. Discussion started: 15 September 2026

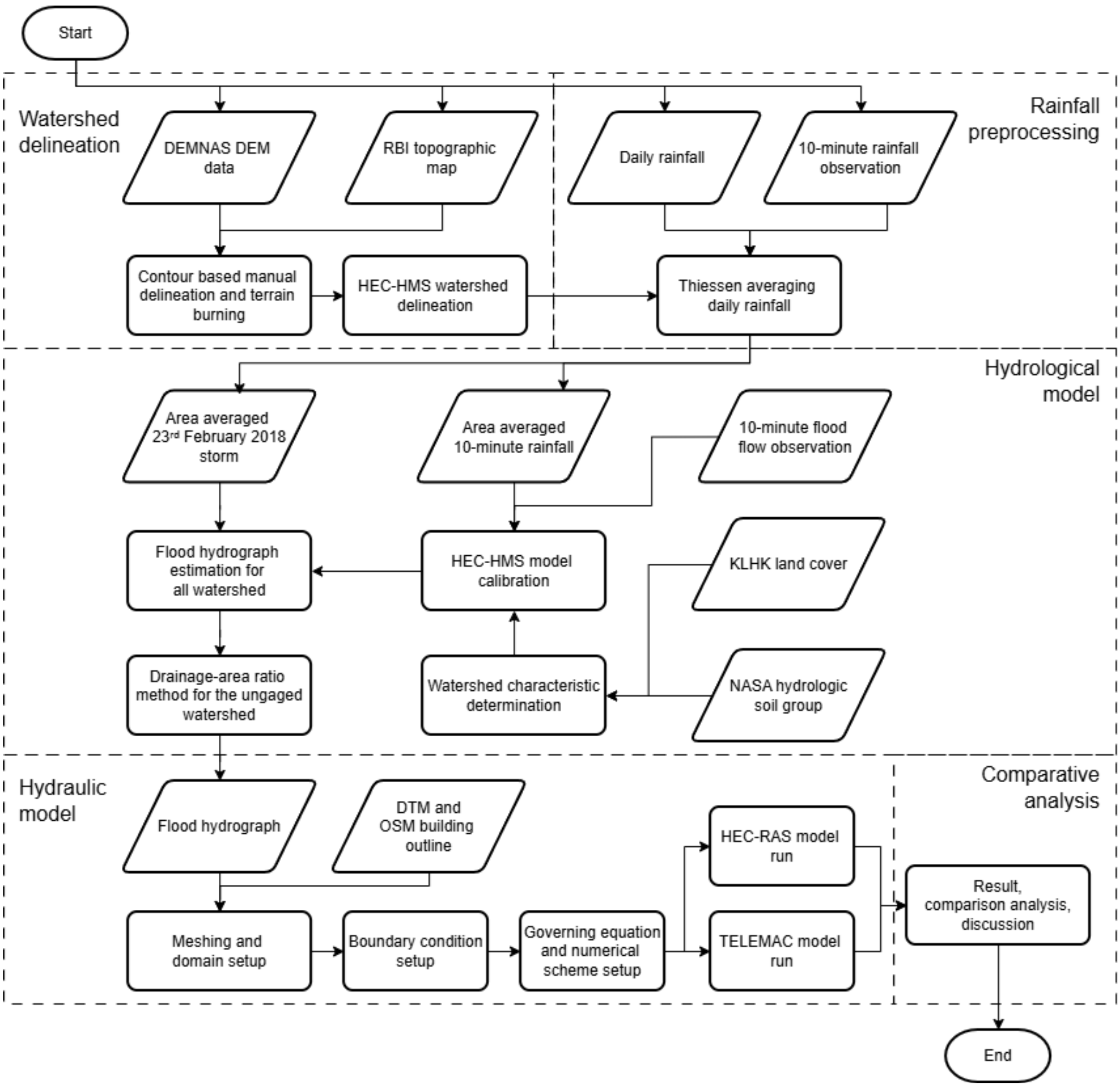

135 **Figure 2: Main flowchart illustrates the methods from watershed delineation, rainfall preprocessing, hydrological model, hydraulic analysis, and comparative analysis.**

2.3.2 Hydrological Analysis

Hydrological analysis was conducted to generate inflow hydrographs for the hydraulic model. It utilized SCS-CN rainfall-runoff method with SCS unit hydrograph. The model's baseline watershed parameters were obtained from land cover and hydrologic soil group data, resulting in a CN value (Soil Conservation Service, 1972) which was calibrated by generating a synthetic hydrograph from a 10-min interval rainfall observation and fitting it to its corresponding observed hydrograph. A

https://doi.org/10.5194/egusphere-2026-4597
Preprint. Discussion started: 15 September 2026

simplified simulation of baseflow and channel routing were also implemented to create a better fit. This model was implemented in all watersheds. We used the drainage-area ratio method (Emerson et al., 2005; Ergen & Kentel, 2016) to convert Citarum headwater streamflow at the Majalaya and Cirasea Gauge into the flow incoming to this Sapan confluence.

2.3.3 Hydraulic Models

The modelling domain is shown Figure 3 (a) and was assigned with a spatially varied Manning friction value: 0.025 for water bodies, 0.035 for rice fields, and 0.06 for residential areas. Both models were simulated using the same outflow's rating curve and flood hydrograph, shown in Figure 3 (b) and (c). Additionally, an outflow boundary condition was assigned to the domain perimeter to simulate realistic floodplain behaviour. Simulation was run for 12 hours with 0.5 seconds adaptive time step in HEC-RAS and 0.2 seconds fixed time step in TELEMAC.

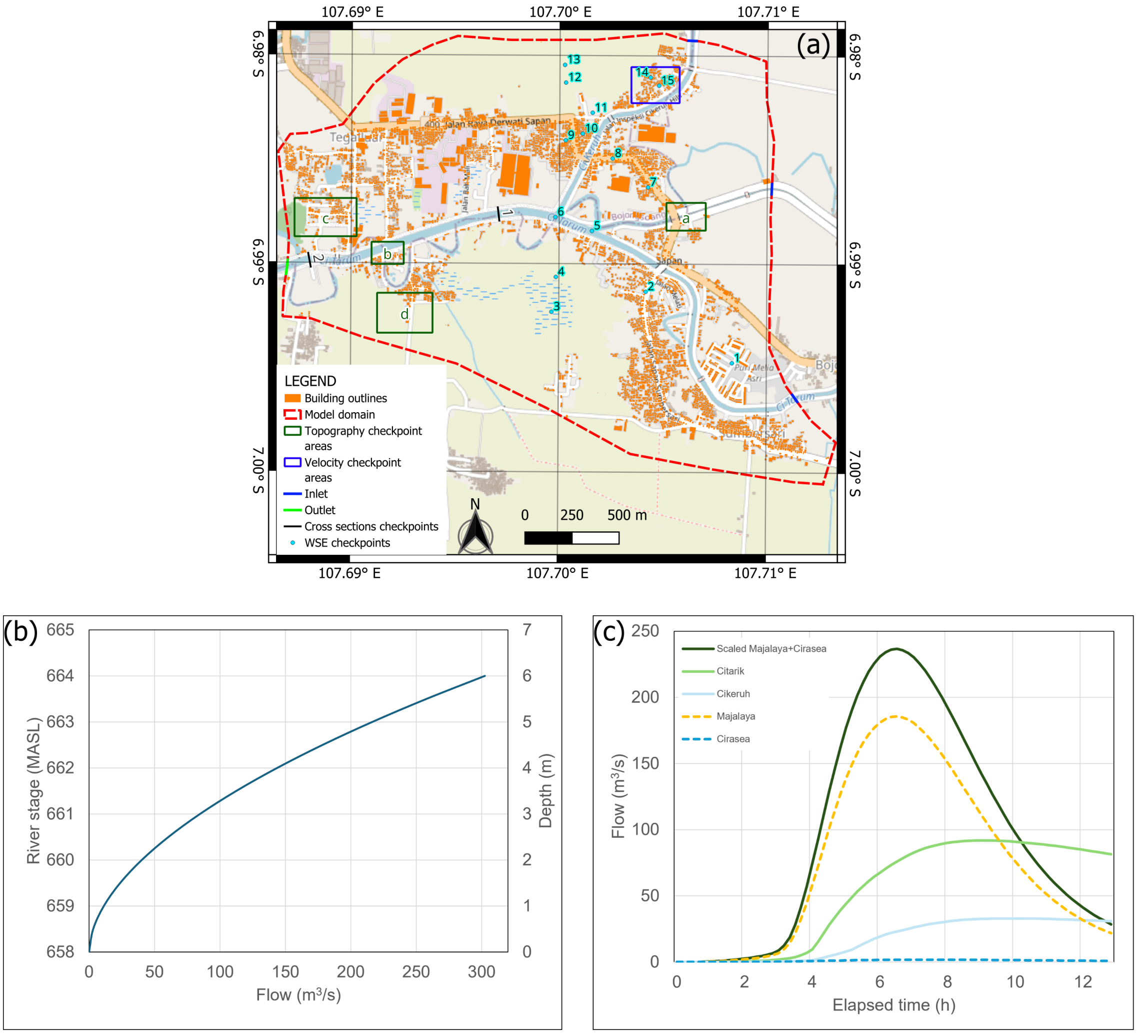

Figure 3: Model domain with the checkpoints and areas to be compared (a), outflow rating curve (b), and inflow hydrographs from the four catchment areas, with Cirasea and Majalaya scaled and combined into one. Base map data provided by ©OpenStreetMap contributors.

Both models solve the continuity equation and shallow water equation, where the latter is a modified, depth averaged Navier-Stokes equation (TELEMAC-2D Software User Manual, 2025; USACE Hydrologic Engineering Center, 2024). HEC-RAS utilizes finite-volume method (FVM) and has three SWE solvers. SWE-ELM (Eulerian-Lagrangian Method) was selected. It utilizes fractional step method where advection and diffusion are solved separately. Advection is solved with a semi-Lagrangian backtrack interpolation, whereas diffusion is solved implicitly. Additionally, HEC-RAS computes hydraulic properties such as hydraulic radius, volume and cross-sectional area from each computational cell that is derived from terrain information, a method that is referred to as subgrid bathymetry (USACE Hydrologic Engineering Center, 2024). On the other

https://doi.org/10.5194/egusphere-2026-4597
Preprint. Discussion started: 15 September 2026

hand, TELEMAC uses FEM and applied fractional step methods. It has multiple options for advection schemes. The N-Edge based Residual Distributive (NERD) scheme was selected which is an explicit advection solver and a part of TELEMAC's residual flux-based distributive scheme that was inspired and derived from explicit finite-volume scheme (Hervouet et al., 2011, 2017). Furthermore, diffusion is also solved implicitly and there is no subgrid bathymetry feature, so it might require finer mesh to read modelling terrain.

Flood models can be improved to portray real life conditions by implementing buildings onto the model's base terrain DEM (Brown et al., 2007; Rohmat et al., 2022; Wulandari et al., 2025; D. Yu & Lane, 2006), an approach referred to as building-by-block approach. Another approach to do this is by using high friction coefficient for the building location, referred as building resistance approach (Mustafa et al., 2023; Mustafa & Szydłowski, 2021) or by making holes on the mesh at each building footprint (Costabile et al., 2023; De Vos, Mahajan, Caviedes-Voullième, & Rüther, 2026; De Vos, Mahajan, Caviedes-Voullième, Rohmat, et al., 2026; Mahajan & De Vos, 2024; Schubert et al., 2008), referred as building-by-holes approach.

HEC-RAS utilized the building-by-block method. It used a coarse 25 m resolution mesh for building areas and open floodplains. Water bodies such as rivers, oxbow lakes, and ponds were assigned with a 5 m resolution finer mesh. Building-by-holes method was implemented in TELEMAC. Open floodplains were also assigned with 25 m resolution mesh. However, finer mesh was applied to areas between buildings. The mesh for this area was made as a function of building-to-building distance and allowed a minimum mesh resolution of 0.5 m (De Vos, Mahajan, Caviedes-Voullième, Rohmat, et al., 2026). The mesh was generated with a Delaunay triangulation mesh generator (Shewchuk, 1996). Water bodies were also assigned with finer mesh resolution: 5 m refinement in the TEL_5 model and 1 m refinement in the TEL_1 model. A summary of each model's setup is shown in Table 2. The differences in building representation and mesh resolution in residential areas and rivers were intentionally implemented to evaluate whether TELEMAC and HEC-RAS could yield similar flood extents with different strategies. For example, Fig. 4 illustrates the different building representations and mesh refinements. TELEMAC's finer mesh should simulate flood propagation effectively. On the contrary, despite the coarser mesh, HEC-RAS' subgrid bathymetry dictates it can simulate flood propagation, even though velocity field simulation might be coarser.

Table 2: Overview and comparison of simulated model scenarios based on their different setups.

Model	Software	River resolution (m)	General resolution (m)	Building refinement	Simulation time (h)	Computing timestep (s)
RAS_5	HEC-RAS	5	25	No	12	0.5 (adaptive)
TEL_5	TELEMAC	5	25	Yes	12	0.2 (fixed)
TEL_1	TELEMAC	1	25	Yes	12	0.2 (fixed)

https://doi.org/10.5194/egusphere-2026-4597
Preprint. Discussion started: 15 September 2026

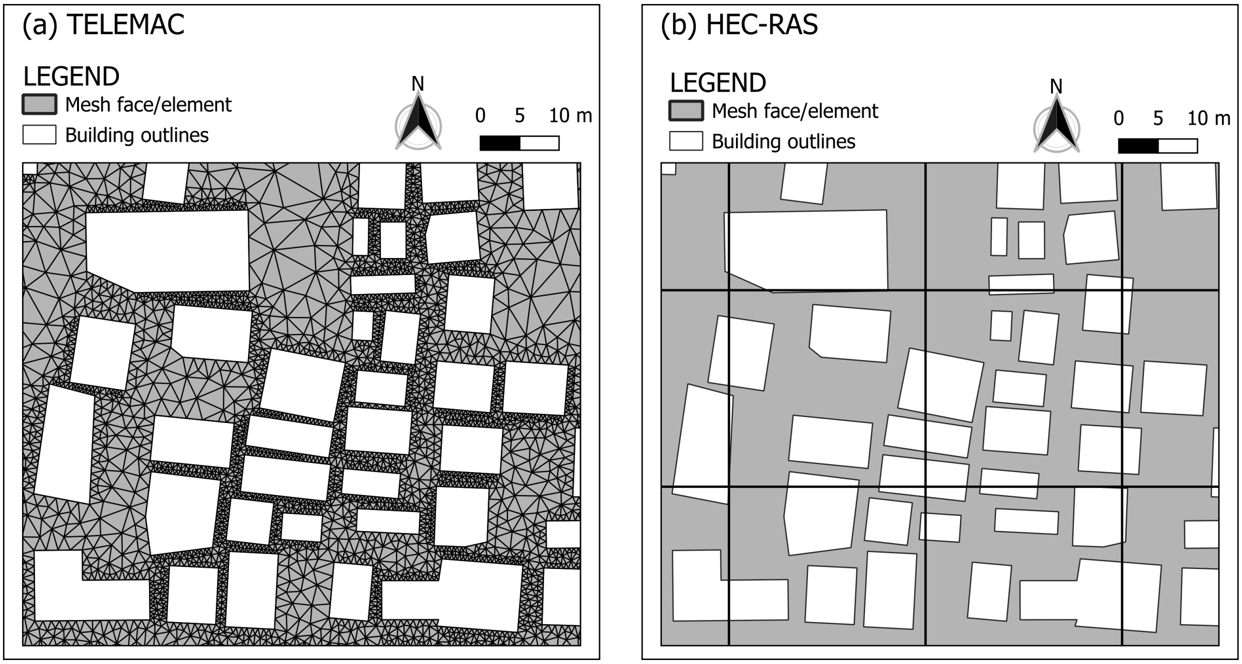

Figure 4: Building representation and meshing comparison in residential areas between (a) TELEMAC and (b) HEC-RAS.

2.3.4 Model Comparison

Comparison focused on flood parameters such as Water Surface Elevation (WSE), max inundated area, and flood propagation. Although water depth is a practical parameter, WSE was selected as the comparable parameter because water depth is dependent on topography which might be slightly different between models. Velocity vectors were examined in detail in some areas. To conduct a more straightforward comparison, max flood extent was taken at a single time step rather than an absolute maximum inundation composite from the entire simulation. Both this flood extent and propagation were compared through visual inspection. Furthermore, the maximum inundated area was also quantified with its magnitude in hectares, and the CSI (Critical Success Index) was computed as shown by Eq. (1), with RAS_5 assumed to be the ground truth reference. It is defined as:

$$CSI = \frac{TP}{TP + FP + NP}, \quad (1)$$

where TP is True Positive, meaning both models predict a flooded cell. FP is False Positive, meaning TELEMAC predicts a flooded cell, but HEC-RAS doesn't. NP is Neutral Positive, where both models predict an unflooded cell.

3 Results and Discussions

RAS_5 solved the simulation for 35052 nodes with 8 cores and an adaptive 0.5 second computational timestep in 21 minutes 39 seconds computing time. TEL_5 solved the simulation for 504385 nodes with 16 cores and 0.2 seconds fixed computational

https://doi.org/10.5194/egusphere-2026-4597
Preprint. Discussion started: 15 September 2026

time step in 15 hours and 50 minutes. TEL_1 solved the simulation for 1099223 nodes also with 16 computational cores and 0.2 seconds fixed timestep in 44 hours and 59 minutes. The finer mesh between buildings required smaller time step as a tradeoff for expected accuracy.

3.1 Flood Extent

Figure 5 shows the inundation t = 11 h, representing the period where max inundation extent was observed across the majority of the domain's floodplain. Comparison metric is shown in Table 3. Visual inspection shows TEL_5 was closer to RAS_5 in areas illustrated by the yellow ellipses numbered I and III in Fig. 5. However, the CSI and relative difference indicated TEL_1 was conversely closer to RAS_5. This was because TEL_5 generated more overtopped spots along the rivers, at area number II for example.

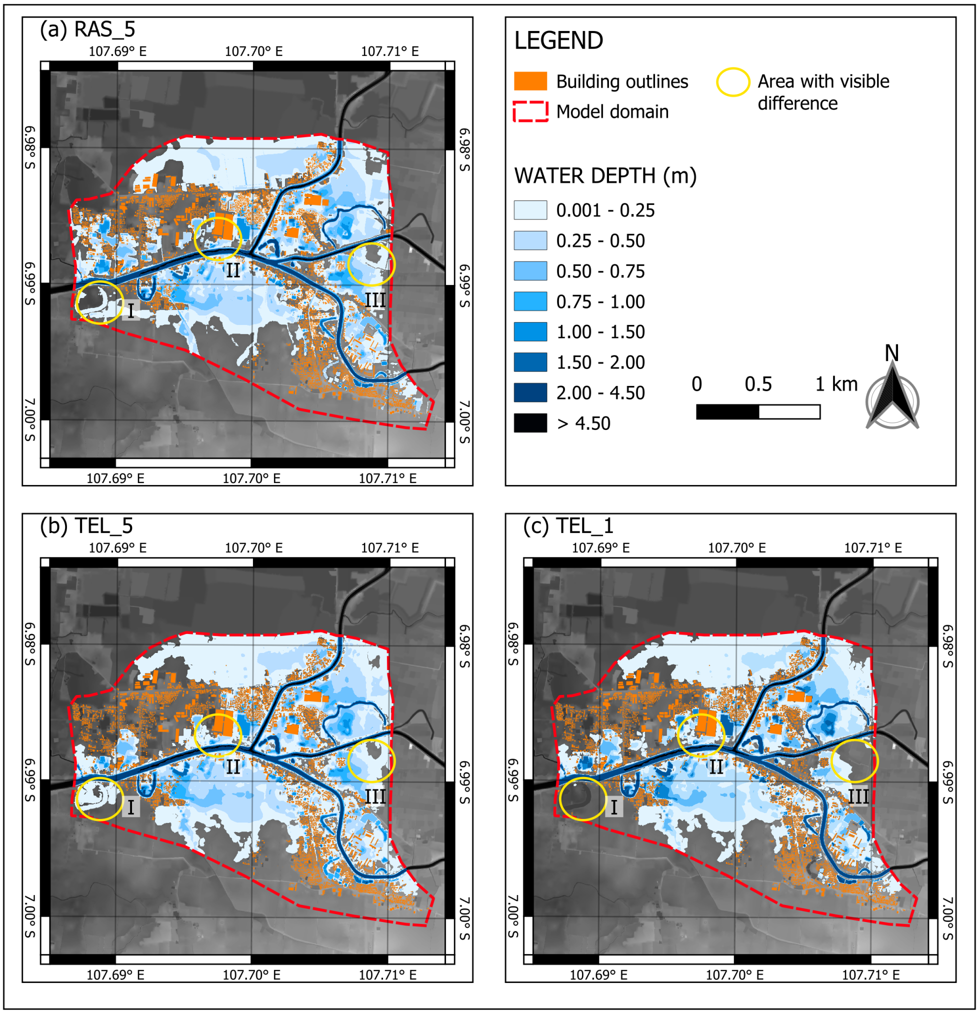

Figure 5: Observed max. inundation taken from RAS_5 (a), TEL_5 (b), and TEL_1 (c) with a DTM as background layer.

https://doi.org/10.5194/egusphere-2026-4597
Preprint. Discussion started: 15 September 2026

Table 3: Comparison metric between each scenario: TEL_5 and TEL_1 relative difference to RAS_5 and CSI value with RAS_5 as benchmark.

Scenario	Inundated area (ha)	Relative difference	CSI
RAS_5	255.08	-	-
TEL_5	279.91	9.28 %	0.788
TEL_1	251.68	1.34 %	0.804

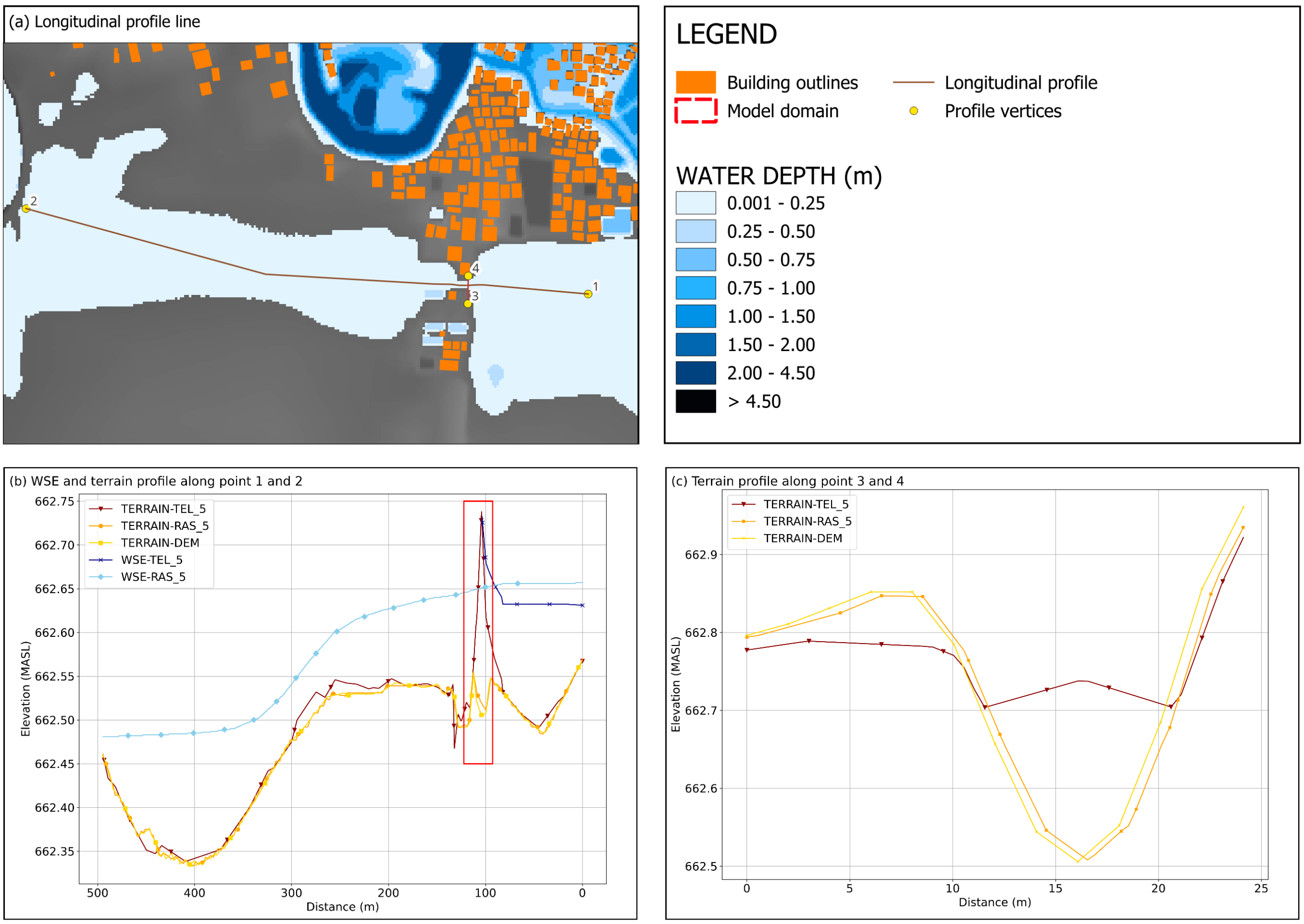

Figure 6: Illustration of TEL_5 and TEL_1's coarse mesh interpolation in floodplain preventing further propagation due to higher averaged terrain compared with RAS_5's subgrid terrain. Figure 6(a) utilizes a DTM as background layer with each profile line position shown.

https://doi.org/10.5194/egusphere-2026-4597
Preprint. Discussion started: 15 September 2026

Another significant overtopping spot was observed in the oxbow lake inside ellipse number I in TEL_5. It managed to match RAS_5's result for the wrong reason, where it was caused by a simulated flood propagation from upstream floodplain through a gap in the terrain, as shown by Fig. 6. TEL_5 and TEL_1 couldn't simulate this with the current mesh setup due to nodal terrain interpolation causing artificially higher averaged terrain elevation. Through the utilization of subgrid bathymetry information, despite the same coarse mesh covering this area, RAS_5 was able to accurately capture floodplain terrain and urban features like road, residential embankments, small crests and troughs, and small drainage channels or ditches with coarse mesh and managed to spread inundation farther. A finer mesh could be implemented in TEL_5 and TEL_1 to match RAS_5's results.

The overtopping spots in TEL_5 were not caused by higher river stage. Fig. 7 shows an example where TEL_5 simulated artificial propagation up and over a riverbank in cross section (XS) number 2. This appeared to be caused by the nodal wetting-drying algorithm of TELEMAC's FEM where a node is intentionally made wet for model stability. The effect was reduced significantly in TEL_1 due to finer mesh on the river. Furthermore, comparing cross sections of each model, as shown in Fig. 8, it was observed that TEL_5's mesh generated a lower riverbank elevation compared to RAS_5. Although the difference was negligible, water could leak earlier to the floodplain and shown as inundated. Despite explicitly aligning the nodes with bank lines so that no elements could bypass the crest, TEL_5 couldn't capture the highest point represented with the same accuracy as TEL_1 because of the smoothing effect from the nodal terrain interpolation that is inherently dependent on the mesh resolution. On the other hand, the effect is not visible in RAS_5 because it can do cell partial wetting (Orozco et al., 2024). This further highlights the need for rigorous mesh refining in TELEMAC.

Despite its advantages and no wetting-drying issue, RAS_5's subgrid bathymetry also generated riverbank leaks and artificial propagation. If a single computational cell simultaneously covers a river, the crest of riverbank, and the adjacent lower elevation terrain, the river stage could bypass the bank, making a flux of water out of the river. This could create premature leaks, adding excessive volume to floodplain, and potentially increasing inundation. Although the same strategy of aligning the cell edges with riverbank lines had been implemented, it yielded the same result, which implies that the cells should be more refined.

Therefore, unlike HEC-RAS, TELEMAC required finer river refinement to get an accurate bathymetry representation, especially regarding its wetting-drying issue. The extra inundation in TEL_5 induced by coarser mesh could be considered negligible but it would be a primary limitation if TEL_5 couldn't represent the actual channel geometry as it would artificially reduce channel conveyance. However, adequate mesh refining isn't limited to TELEMAC. Despite RAS_5's utilization of subgrid bathymetry, it still requires fine mesh to accurately simulate flows around steep topographic gradients along the riverbanks.

https://doi.org/10.5194/egusphere-2026-4597
Preprint. Discussion started: 15 September 2026

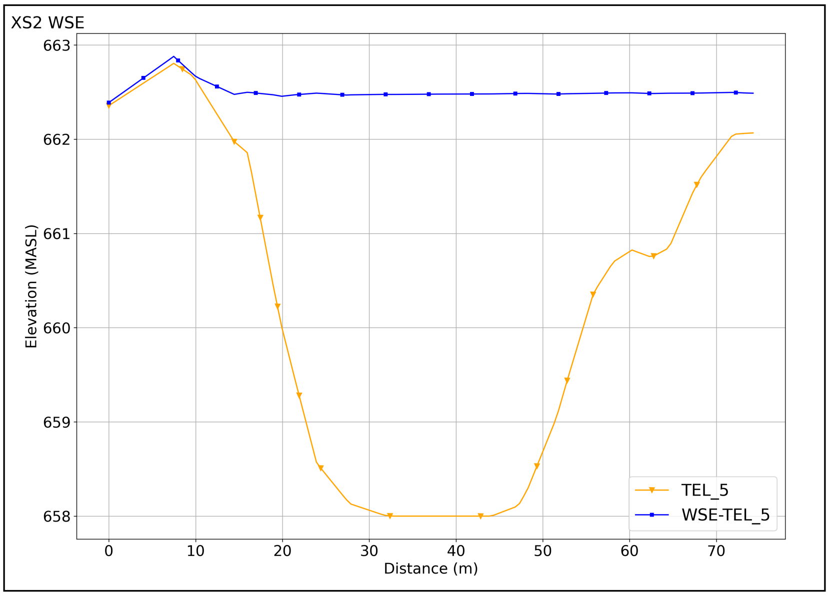

Figure 7: River WSE and its bathymetry extracted from TEL_5 in XS2 with visible water propagating up the riverbank with depth of 0.0085 m.

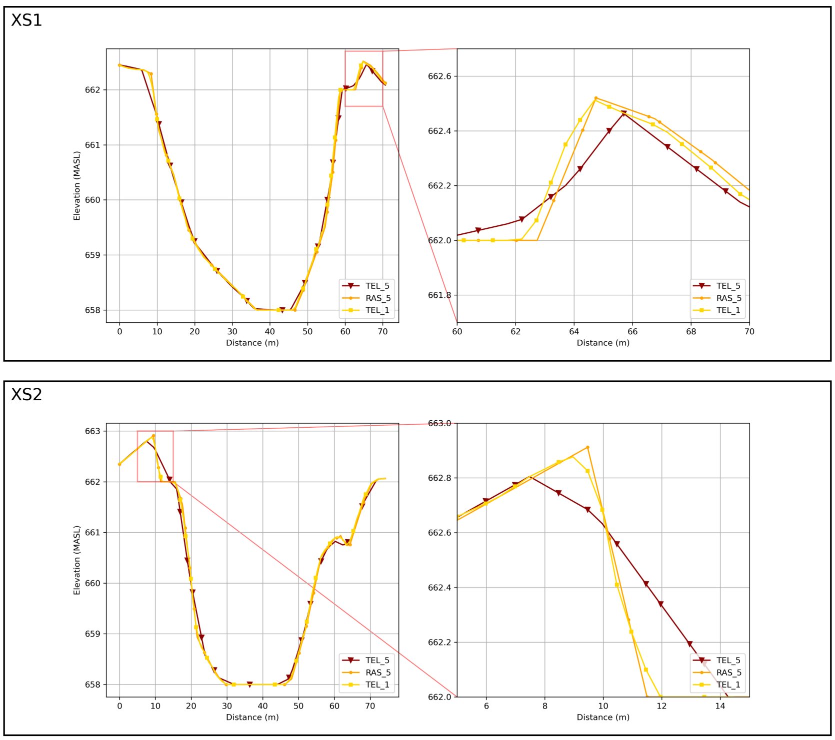

Figure 8: Comparison of river cross section bathymetry interpolated to the mesh between RAS_5, TEL_5, and TEL_1, respectively at cross section number 1 and 2.

https://doi.org/10.5194/egusphere-2026-4597
Preprint. Discussion started: 15 September 2026

3.2 Flood propagation

Only TEL_1's propagation was compared with RAS_5 given that its bathymetry representation is closely aligned with RAS_5. Fig. 9 shows flood extent from simulation time 05:00, 05:30, and 06:00 while Fig. 10 shows flood extent from simulation time 06:30, 07:00, 08:00, and 10:00.

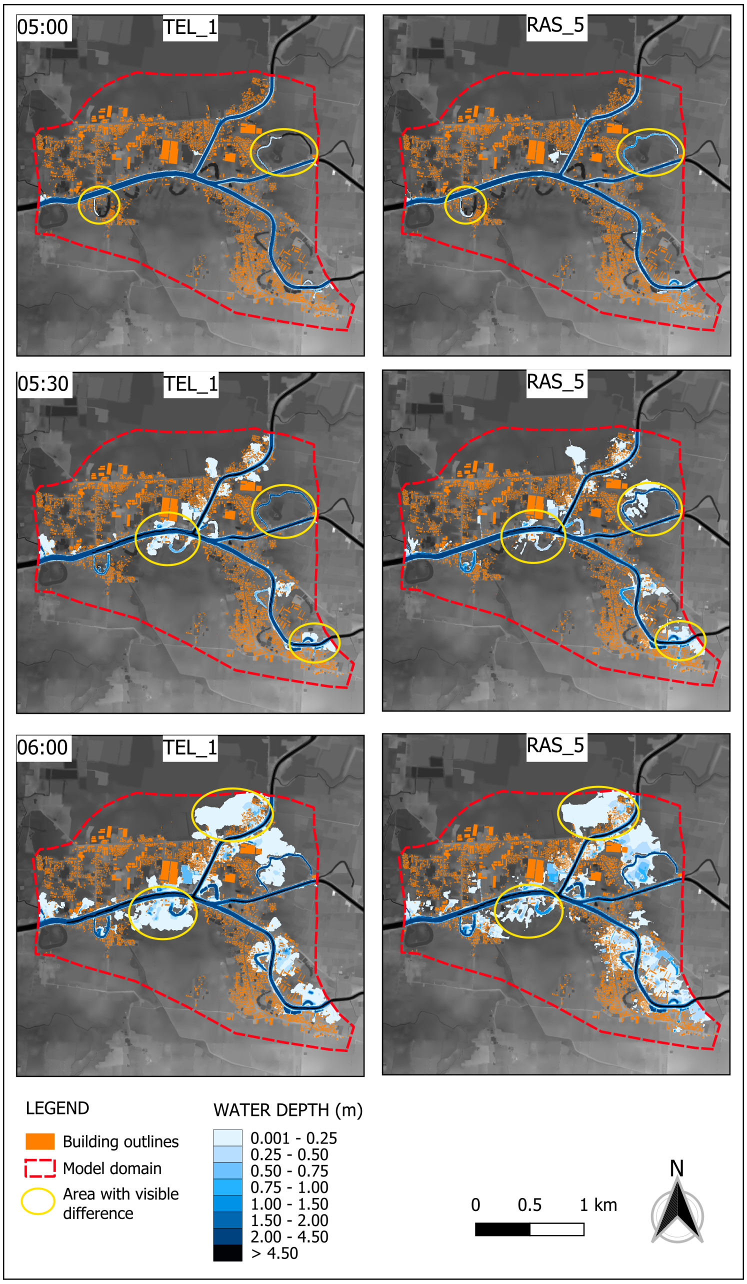

Figure 9: Flood propagation with comparison between TEL_1 (left) and RAS_5 (right) at t = 5.0 h, 5.5 h, and 6.0 h with DTM background.

https://doi.org/10.5194/egusphere-2026-4597
Preprint. Discussion started: 15 September 2026

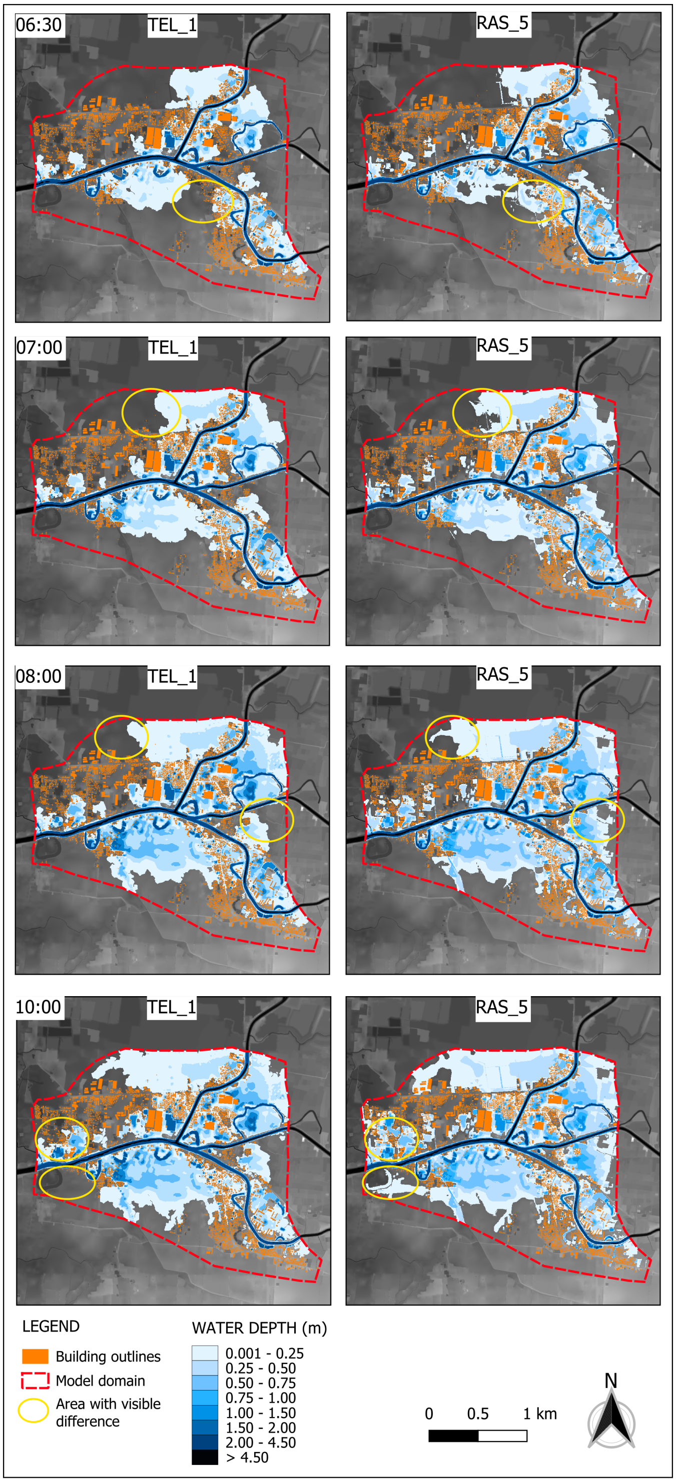

275 **Figure 10: Flood propagation comparison between TEL_1 (left) and RAS_5 (right) at t = 6.5 h, 7.0 h, 8.0 h, and 10.0 h, with DTM background.**

https://doi.org/10.5194/egusphere-2026-4597
Preprint. Discussion started: 15 September 2026

At 05:00, there was no major simulated inundation. Although negligible, RAS_5 simulated higher river WSE at Citarum from its inlet to the Citarik confluence and could serve as a contributor to propagation in later time steps. However, the pattern changed downstream, as shown in Fig. 11. The initially lower WSE could be caused by the way the inflow boundary in RAS_5 is governed by normal depth whereas in TEL_1 it is a free inflow or could also be caused by TEL_1's finer mesh outperforming RAS_5's subgrid information and captured a more realistic bathymetry. Furthermore, although the outflow boundary condition utilized the same rating curve, it might serve as another contributor to the different WSE near the outflow boundary condition as the two models could handle it differently. Furthermore, RAS_5 simulated early flooding of oxbows, as shown with Fig. 12 (a) and (b), which shows how a higher topography gets bypassed. Although it was minor, this could happen because of the terrain skipping issue. It was capturing the river-oxbow connection in detail, but the coarse mesh didn't correctly simulate how water would move between cells.

At 05:30, the longitudinal river WSE profile remained as shown in Fig. 11, and looking at Fig. 9, both models now simulated overtopping oxbows. Additionally, the river WSE profile could cause RAS_5 to overtop more water in upstream side of Citarum, specifically near the inflow, whereas TEL_1 overtopped more water in Citarum after the confluence. The terrain skipping in riverbank could also contribute.

At 06:00, the overtopping spots grew larger to inundate more areas. The longitudinal river WSE profile remained but started to equalize. TEL_1's inundation on upstream Cikeruh right side (indicated with blue box in Fig. 3), particularly in and after the building complex had similar inundations to RAS_5. Theoretically, the finer mesh between buildings would mean a better building representation and should dictate a slower propagation. Fig. 13 shows TEL_1 simulated how floods flow between buildings. However, RAS_5 generated velocity fields that point towards the general direction of the flood flow and disregarding the building footprints. Despite this, RAS_5 managed to distribute inundation around buildings through the utilization of subgrid bathymetry. The velocity fields could become a clue that the flood waves were being more damped in TEL_1, although it might be visually negligible.

https://doi.org/10.5194/egusphere-2026-4597
Preprint. Discussion started: 15 September 2026

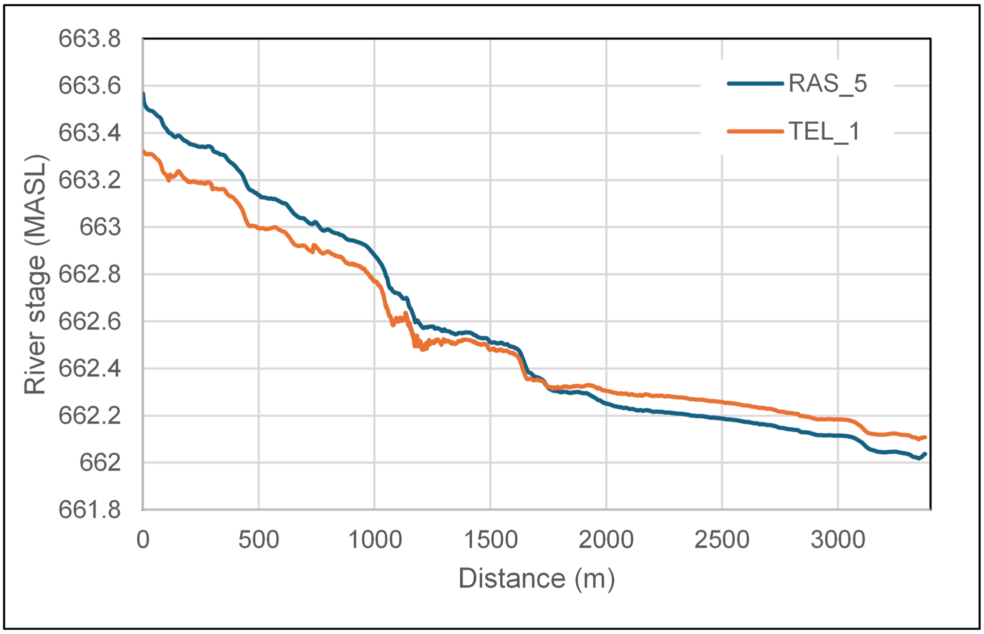

Figure 11: Longitudinal Citarum stage profile of RAS_5 and TEL_1 at simulation t= 5.0 h.

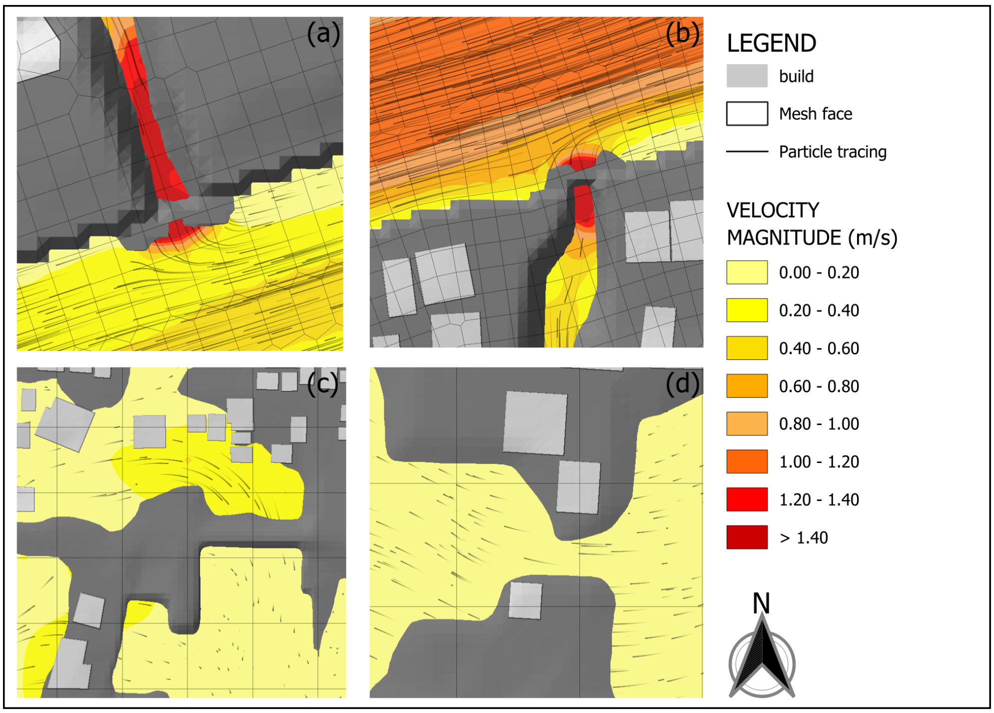

Figure 12: Snapshots of topography evaluation areas that shows HEC-RAS' particle tracing (streamline) skipping high terrains shown with the DTM background layer (a, b, c) and capturing topographical gap (d).

https://doi.org/10.5194/egusphere-2026-4597
Preprint. Discussion started: 15 September 2026

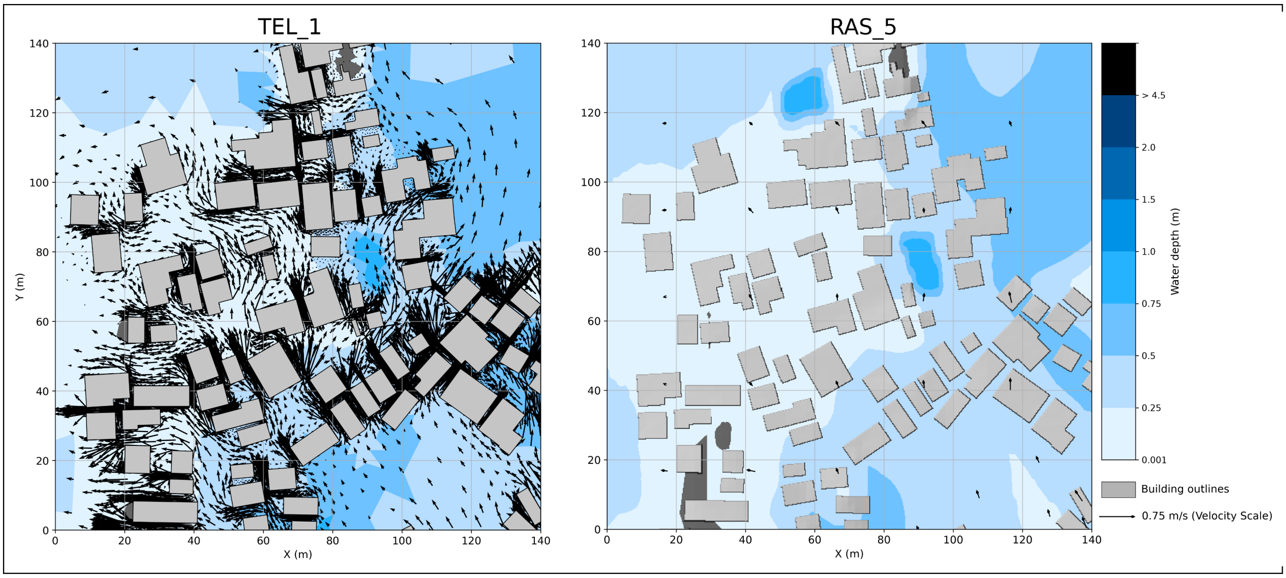

Figure 13: Velocity vectors around building comparison between TELEMAC (left) and HEC-RAS (right).

At 06:30, as shown by Fig. 10, the flood waves from Citarum left bank before and after the confluence now had joined in RAS_5. This hadn't occurred yet in TEL_1. The flood wave from the spot before the confluence wasn't as big as RAS_5 and it arrived late. But the flood wave from the spot after the confluence was bigger in TEL_1 which could be caused by the higher river WSE.

At 07:00, the flood waves in Citarum's left side had combined, creating a similar inundation area between RAS_5 and TEL_1 despite the different overtopping and propagation mechanisms. The inundation in Citarik's right side also became identical between the two models. At 08:00, only the edges of the flood waves differ. Subsequently, at 10:00, flood propagation edges discrepancy now got more identified. Fig. 12 (d) and Fig. 7 show only RAS_5 simulated flood flow through a gap in a higher ground as explained before. However, it also caused artificial propagation due to the terrain skipping issue, as shown at Fig. 12 (c), where the coarse cells ignored urban features like pools and embankments. Overall, the propagation mechanism further supported all the differences found when comparing max. inundated area. Ultimately, the primary determining factors were building representation and meshing architecture, further influenced with subgrid bathymetry in RAS_5.

3.3 WSE Checks

Table 4 shows the maximum WSE generated at all checkpoints shown in Fig. 3 and its difference between TEL_1 and RAS_5. Despite its negligible discrepancy, its location could further support the findings that have been mentioned. Points 5 and 6 are at a river. Point 1, 2, 7, 8, 9, 10, 14, and 15 are in residential areas, with points 9, 10, 14, and 15 having denser building. Point 3, 4, 11, 12, and 13 are on flat rice fields with no buildings. Noticeably, despite having different mesh refinement, the WSE of point 5 and 6 on a confluence point were similar. In floodplains at point 3 and 4, both had similar WSE, indicating that the inundations were identical, despite different propagation mechanisms. However, points 12 and 13 were higher in RAS_5 and

https://doi.org/10.5194/egusphere-2026-4597
Preprint. Discussion started: 15 September 2026

could be caused by the propagation that is less damped or from the domain perimeter boundary condition holding more water. Point 15, which stands before the dense building, had higher WSE in TEL_1 than in RAS_5. But inside and around the building complex at point 14, WSE in TEL_1 is lower than in RAS_5, which could indicate that the flood was damped in TEL_1. Moving to other building complexes, point 1 has higher WSE in RAS_5 because it was flooded earlier. TEL_1 was higher in point 2, which could also be a clue of a more damped flood. Points 7 and 8, as well as 9 and 10, were similar.

This WSE comparative analysis highlighted how RAS_5 and TEL_1 generated similar inundation profile in terms of depth. This further clarified HEC-RAS coarse mesh' ability to distribute water between buildings. The major discrepancies ultimately could arise from different propagation and flood damping from building representation, although visually and timewise it looked similar. The domain perimeter which utilizes different outflow boundary condition systems could also be a contributor. Furthermore, as shown previously on Fig. 11, river WSE profile discrepancy was observed only near the inflow and outflow boundary condition which could indicate as another evidence that they were one of the contributing factors.

Table 4: Comparison of WSE and its calculated differences at all checkpoints between TEL_1 and RAS_5.

Point	TEL_1	RAS_5	Delta
1	663.03	662.34	0.690
2	663.09	663.06	0.030
3	662.74	662.73	0.010
4	662.74	662.73	0.010
5	662.89	662.90	-0.010
6	662.81	662.81	0.000
7	662.83	662.83	0.000
8	662.82	662.82	0.000
9	662.81	662.80	0.010
10	662.82	662.81	0.010
11	662.39	662.39	0.000
12	662.18	662.24	-0.060
13	662.20	662.23	-0.030
14	662.46	662.49	-0.030
15	662.74	662.62	0.120

https://doi.org/10.5194/egusphere-2026-4597
Preprint. Discussion started: 15 September 2026

3.4 Limitations

There is no observation data for comparison with ground truth in this research. This study only concluded how each result differs. The simulations were also conducted in urban areas with multiple overtopping spots which increases the complexity of comparison in dense building areas. For a more in-depth assessment of model accuracy, a smaller scale physical model could be implemented to serve as a ground truth, allowing a direct comparison of both model's performance at generating realistic physical results (Z. Li et al., 2019; Mustafa & Szydłowski, 2021).

Furthermore, this study only compared one scenario of floods. The models might behave differently with different return period scenarios. There are also other scenarios that can be evaluated such as levee breach or dam break, which can be done by both HEC-RAS and TELEMAC (Khanal et al., 2025; H. Yu et al., 2025). Because it generates higher velocity of flow, it might provide a comparison of how each model handles rapid flood propagation around buildings.

Some model setups in this study were also deliberately made differently to see how it would affect the result. Even though the results were relatively similar, the simulation setup could be made fairer. For example, using depth governed inflow for TELEMAC to mimic HEC-RAS' normal depth governed inflow and implementing finer mesh if necessary to prevent artificial leakage and propagation. Modelling domain could also be extended so that flood waves interact less with the domain perimeter boundary condition.

4 Conclusion

Flooding is a worldwide problem whose risk needs to be mitigated. Two-dimension hydrodynamic model has grown to be a widely used tool to simulate flood. This tool, together with building integration, was implemented in Sapan, Upper Citarum Watershed using HEC-RAS and TELEMAC. HEC-RAS had 5 m river refinement (RAS_5), whereas TELEMAC had two versions with 5 m (TEL_5) and 1 m (TEL_1) river refinement. The used flood flow was a historical event on 23rd of February 2018, generated from a calibrated hydrological model. Analysis revealed that while both models generated relatively similar results, discrepancies persisted. TEL_5 couldn't acquire an accurate river bathymetry representation achieved by RAS_5, inducing excessive overtopping and influenced by wetting-drying algorithms, although the quantitative impact was negligible. TEL_1 didn't have this issue due to its finer bathymetry representation. Despite having coarser mesh, RAS_5 managed to simulate flood inundation distributed around buildings. However, the generated velocity vectors ignored these building features, which indicated less damped flood waves and didn't simulate interaction between buildings achieved by TEL_1 and TEL_5. Furthermore, unlike TEL_5 and TEL_1, RAS_5's coarse floodplain cells were able to capture urban features like drainage ditches and gaps between embankments which contributed to be another driver of different flood extent. However, this also caused premature and artificial leaks between rivers and floodplains due to a cell simultaneously capturing high and low elevation terrain, which caused an effect of terrain skipping. It can be concluded that RAS_5 can be used for broad-scale flood models whose depth is the main concern, for example, at urban flat floodplains in downstream areas. However, if the main concern is the flow velocity around buildings or structures, TELEMAC can be an alternative, especially for areas who

https://doi.org/10.5194/egusphere-2026-4597
Preprint. Discussion started: 15 September 2026

are more prone to flash floods. Another important thing to note is that the flood propagation in this study is based on natural rivers with flood events that are not recorded. Further studies involving a simpler physical river model and numerical model as comparison would further explain the difference between HEC-RAS and TELEMAC.

Data availability

The datasets, model input files, model configurations, and simulation outputs used in this study are publicly available through Zenodo at doi.org/10.5281/zenodo.21674085.

Author contributions

ANA: conceptualization, formal analysis, investigation, methodology, software, visualization, writing – original draft. LFDV: conceptualization, investigation, methodology, resources, supervision, writing – review and editing. FIWR: conceptualization, data curation, investigation, methodology, resources, supervision writing – reviewing and editing. MSBK: conceptualization, investigation, project administration, supervision.

Competing interests

The authors declare that they have no conflict of interest.

Acknowledgements

The authors gratefully acknowledge the Balai Besar Wilayah Sungai (BBWS) Citarum for their continuous collaboration and valuable support throughout this study, including assistance with hydrological data acquisition and technical discussions.

Financial support

This research was supported by Institut Teknologi Bandung (ITB), Program Riset Unggulan ITB under Contract No FTSL.PN-6-212-2026.

References

Abusyarif, A. R., Wardhana, P. N., and Sulistiono, B.: Preliminary simulation of series groyne in upstream reach of Klambu Barrage in Jawa Tengah Indonesia, in: The 2nd International Symposium on Civil, Environmental, and Infrastructure Engineering, Yogyakarta, Indonesia, 10 August 2022, AIP Conf. Proc., 2846, https://doi.org/10.1063/5.0154339, 2023.

https://doi.org/10.5194/egusphere-2026-4597
Preprint. Discussion started: 15 September 2026

Adeke, D. P. and Mugume, S. N.: A methodology for development of flood-depth-velocity damage functions for improved estimation of pluvial flood risk in cities, J. Hydrol., 653, 132736, https://doi.org/10.1016/j.jhydrol.2025.132736, 2025.

Al-Hussein, A. A. M., Kadhim, E. J., Mahmood, B. F., Sulaiman, M. A. M., and Bouri, S.: Application of the HEC-RAS 2D model for flood hazard modeling and analysis: Focus on Duhok City, Kurdistan Region of Iraq, Phys. Chem. Earth, 143, 104345, https://doi.org/10.1016/j.pce.2026.104345, 2026.

Aminah, S., Riawan, E., Syahputra, M. R., and Kuntoro, A. A.: Identification of Extreme Precipitation Changes Due to Climate Change in Indonesia, in: Proceedings of the International Conference on Radioscience, Equatorial Atmospheric Science and Environment and Humanosphere Science, 849–857, https://doi.org/10.1007/978-981-97-0740-9_75, 2024.

Angelakis, A. N., Capodaglio, A. G., Valipour, M., Krasilnikoff, J., Ahmed, A. T., Mandi, L., Tzanakakis, V. A., Baba, A., Kumar, R., Zheng, X., Min, Z., Han, M., Turay, B., Bilgiç, E., and Dercas, N.: Evolution of Floods: From Ancient Times to the Present Times (ca 7600 BC to the Present) and the Future, Land, 12, 1211, https://doi.org/10.3390/land12061211, 2023.

Avila-Aceves, E., Plata-Rocha, W., Monjardin-Armenta, S. A., and Rangel-Peraza, J. G.: Geospatial modelling of floods: a literature review, Stoch. Environ. Res. Risk Assess., 37, 4109–4128, https://doi.org/10.1007/s00477-023-02505-1, 2023.

Badan Informasi Geospasial: Digital Elevation Model Nasional (DEMNAS), BIG [data set], tanahairindonesia.go.id, last access: 28 July 2026, 2018.

Badan Informasi Geospasial: Rupa Bumi Indonesia (RBI), BIG [data set], tanahairindonesia.go.id, last access: 28 July 2026, 2019.

Bhattarai, Y., Bista, S., Talchabhadel, R., Duwal, S., and Sharma, S.: Rapid prediction of urban flooding at street-scale using physics-informed machine learning-based surrogate modelling, Total Environ. Adv., 12, 200116, https://doi.org/10.1016/j.teadva.2024.200116, 2024.

Badan Nasional Penanggulangan Bencana: Data Informasi Bencana Indonesia (DIBI), BNPB [data set], dibi.bnpb.go.id, last access: 28 July 2026, 2026.

Cea, L. and Costabile, P.: Flood Risk in Urban Areas: Modelling, Management and Adaptation to Climate Change – A Review, Hydrology, 9, 50, https://doi.org/10.3390/hydrology9030050, 2022.

Cheng, X., Cheng, L., Wu, S., Zhang, J., Li, Y., Lei, X., Wu, K., and Liu, P.: A comparative assessment of human entrapment and instability risks in flash floods, J. Environ. Manage., 400, 128761, https://doi.org/10.1016/j.jenvman.2026.128761, 2026.

Costabile, P., Costanzo, C., Kalogiros, J., and Bellos, V.: Toward Street-Level Nowcasting of Flash Floods Impacts Based on HPC Hydrodynamic Modeling at the Watershed Scale and High-Resolution Weather Radar Data, Water Resour. Res., 59, e2023WR034599, https://doi.org/10.1029/2023WR034599, 2023.

De Vos, L. F., Mahajan, K., Caviedes-Voullième, D., Rohmat, F., Adiprayoga, M. F., and Rüther, N.: Efficient and Automated Mesh Generation for Refined Flood Modeling in Complex Urban Environments, EGU General Assembly 2026, Vienna, Austria, https://doi.org/10.5194/egusphere-egu26-11573, 2026.

https://doi.org/10.5194/egusphere-2026-4597
Preprint. Discussion started: 15 September 2026

De Vos, L. F., Mahajan, K., Caviedes-Voullième, D., and Rüther, N.: Culvert blockages in 2D-hydrodynamic flash flood modeling: quantifying the impact on flood dynamics and mitigation strategies, Nat. Hazards Earth Syst. Sci., 26, 2319–2352, https://doi.org/10.5194/nhess-26-2319-2026, 2026.

Emerson, D. G., Vecchia, A. V., and Dahl, A. L.: Evaluation of drainage-area ratio method used to estimate streamflow for the Red River of the North Basin, North Dakota and Minnesota, U.S. Geological Survey Sci. Investig. Rep. 2005–5017, https://doi.org/10.3133/sir20055017, 2005.

Enu, K. B., Merk, F., Su, H., Rauch, M., Zingraff-Hamed, A., Broich, K., Förster, K., Pauleit, S., and Disse, M.: A scenario-based analysis of wetlands as nature-based solutions for flood risk mitigation using the TELEMAC-2D model, Nature-Based Solutions, 7, 100236, https://doi.org/10.1016/j.nbsj.2025.100236, 2025.

Ergen, K. and Kentel, E.: An integrated map correlation method and multiple-source sites drainage-area ratio method for estimating streamflows at ungauged catchments: A case study of the Western yellow Sea Region, Turkey, J. Environ. Manage., 166, 309–320, https://doi.org/10.1016/j.jenvman.2015.10.036, 2016.

Farid, M., Tsamara Dewi, N., Oktariyanto Nugroho, E., Bagus Adityawan, M., Alhamid, A. K., Wahid, A. N., Gunawan, W. C., Javas, J., and Permana, M. F.: Development of an empirical flood fragility curve for levee failure and its application in probabilistic flood risk assessment: A case study of Citeureup Village, Indonesia, Int. J. Disaster Risk Reduct., 133, 105793, https://doi.org/10.1016/j.ijdrr.2025.105793, 2026.

Feng, Q., Kim, D., Wang, W., Lee, J., Kim, K., and Kim, H. S.: A Case Study: Evaluation of Urban Flood Resilience Based on Fuzzy Mathematics and VIKOR Method in Ulsan Metropolitan City, South Korea, KSCE J. Civ. Eng., 28, 1554–1565, https://doi.org/10.1007/s12205-024-0595-5, 2024.

García Martínez, M., Osornio Berthet, L. J., Meléndez Estrada, J., and Cruz Castro, O.: Identification of flood-prone areas using the HEC-RAS 2D model in a region of the Valley of Mexico, Chemosphere, 386, 144609, https://doi.org/10.1016/j.chemosphere.2025.144609, 2025.

Handyastono, B., Alghoul, M. A., Rizki, A., Djambek, N. P., Kusuma, M. S. B., Kuntoro, A. A., Harlan, D., Nugroho, E. O., Munthe, H. M., Hazmi, M., Wisanggeni, D. H., and Rizqy, M. A.: Flood hazard assessment in Pemaluan Village due to land use change in IKN (Ibu Kota Nusantara) as the New Capital City of Indonesia, Case Stud. Chem. Environ. Eng., 11, 101211, https://doi.org/10.1016/j.cscee.2025.101211, 2025.

Hervouet, J.-M., Pavan, S., and Ricchiuto, M.: Residual distribution advection schemes in TELEMAC, Inria Research Report No. 9087, https://inria.hal.science/hal-01571827v2, 2017.

Hervouet, J.-M., Razafindrakoto, E., and Villaret, C.: Dealing with dry zones in free surface flows: a new class of advection schemes, in: Proceedings of the 34th IAHR World Congress, 4103–4110, 2011.

Houngue, N. R., Almoradie, A. D. S., Thiam, S., Komi, K., Adounkpè, J. G., Begedou, K., and Evers, M.: Climate and Land-Use Change Impacts on Flood Hazards in the Mono River Catchment of Benin and Togo, Sustainability, 15, 5862, https://doi.org/10.3390/su15075862, 2023.

https://doi.org/10.5194/egusphere-2026-4597
Preprint. Discussion started: 15 September 2026

Isma, F., Kusuma, M. S. B., Nugroho, E. O., and Adityawan, M. B.: Flood hazard assessment in Kuala Langsa village, Langsa City, Aceh Province, Indonesia, Case Stud. Chem. Environ. Eng., 10, 100861, https://doi.org/10.1016/j.cscee.2024.100861, 2024.

Kardhana, H., Solehudin, Wijayasari, W., and Rohmat, F. I. W.: Assessing basin-wide soil erosion in the Citarum watershed using the USLE method, Results Eng., 22, 102130, https://doi.org/10.1016/j.rineng.2024.102130, 2024.

Kesserwani, G.: Topography discretization techniques for Godunov-type shallow water numerical models: a comparative study, J. Hydraul. Res., 51, 351–367, https://doi.org/10.1080/00221686.2013.796574, 2013.

Khanal, P., Paudel, S., Neupane, R., Adhikari, S., Shrestha, P., Regmi, R. K., Dahal, S., Cho, H., and Marasini, U.: Dam break analysis of the Nagmati and Dhap dams using HEC-RAS, H2Open J., 8, 139–156, https://doi.org/10.2166/h2oj.2025.058, 2025.

Khatooni, K., Hooshyaripor, F., MalekMohammadi, B., and Noori, R.: A new approach for urban flood risk assessment using coupled SWMM–HEC-RAS-2D model, J. Environ. Manage., 374, 123849, https://doi.org/10.1016/j.jenvman.2024.123849, 2025.

Li, C., Sun, N., Lu, Y., Guo, B., Wang, Y., Sun, X., and Yao, Y.: Review on Urban Flood Risk Assessment, Sustainability, 15, 765, https://doi.org/10.3390/su15010765, 2022.

Li, Z., Liu, J., Mei, C., Shao, W., Wang, H., and Yan, D.: Comparative Analysis of Building Representations in TELEMAC-2D for Flood Inundation in Idealized Urban Districts, Water, 11, 1840, https://doi.org/10.3390/w11091840, 2019.

Luo, H. Y., Fan, R. L., Wang, H. J., and Zhang, L. M.: Physics of building vulnerability to debris flows, floods and earth flows, Eng. Geol., 271, 105611, https://doi.org/10.1016/j.enggeo.2020.105611, 2020.

Mahajan, K. and De Vos, L. F.: Assessment of different building representations in numerical urban flood modeling, EGU General Assembly 2024, Vienna, Austria, https://doi.org/10.5194/egusphere-egu24-15865, 2024.

Milanesi, L., Pilotti, M., Belleri, A., Marini, A., and Fuchs, S.: Vulnerability to Flash Floods: A Simplified Structural Model for Masonry Buildings, Water Resour. Res., 54, 7177–7197, https://doi.org/10.1029/2018WR022577, 2018.

Mustafa, A. and Szydłowski, M.: Application of different building representation techniques in HEC-RAS 2-D for urban flood modeling using the Toce River experimental case, PeerJ, 9, e11667, https://doi.org/10.7717/peerj.11667, 2021.

Mustafa, A., Szydłowski, M., Veysipanah, M., and Hameed, H. M.: GIS-based hydrodynamic modeling for urban flood mitigation in fast-growing regions: a case study of Erbil, Kurdistan Region of Iraq, Sci. Rep., 13, 8935, https://doi.org/10.1038/s41598-023-36138-9, 2023.

Nurrokhman, A., Hudalah, D., Zulkaidi, D., and Wijaya, N.: The Impact of Poverty on Urban Sprawl in Developing Countries: A Case Study of the Jakarta Metropolitan Area, Geographies, 6, 18, https://doi.org/10.3390/geographies6010018, 2026.

Oktaviani, A. D., Sahdarani, D. N., Prayoga, J. J., Indraswari, A. O., and Haris, A.: Flood deposits characterization in Citarum Riverbank Area in Bandung Regency, West Java, Indonesia, IOP Conf. Ser.: Earth Environ. Sci., 846, 012006, https://doi.org/10.1088/1755-1315/846/1/012006, 2021.

OpenStreetMap: OSM Buildings, OpenStreetMap [data set], https://osmbuildings.org, last access: 28 July 2026, 2025.

https://doi.org/10.5194/egusphere-2026-4597
Preprint. Discussion started: 15 September 2026

Orozco, A. N. R., Bertrand, N., Pheulpin, L., Migaud, A., and Abily, M.: Comparison Between HEC-RAS and TELEMAC-2D Hydrodynamic Models of the Loire River, Integrating Levee Breaches, in: River Flow 2024, 41–55, https://doi.org/10.1007/978-981-97-4072-7_3, 2024.

Prawirakusuma, A.: Flood Characteristics in the Lower Citarum River, Indonesia and Their Possible Management Practices, Int. J. GEOMATE, 25, https://doi.org/10.21660/2023.111.3993, 2023.

Rohmat, F. I. W., Harjupa, W., Rohmat, D., and Rohmat, F. I. W.: The impacts of global atmospheric circulations on the water supply in select watersheds in the Indonesian Maritime Continent using SPI, Heliyon, 9, e15604, https://doi.org/10.1016/j.heliyon.2023.e15604, 2023.

Rohmat, F. I. W., Löhr, A. J., Pratama, F., Burnama, N. S., and Kuntoro, A. A.: Quantifying time-dependent flood resilience index in a densely populated urban environment in Manado, Indonesia, Int. J. Disaster Risk Reduct., 116, 105112, https://doi.org/10.1016/j.ijdrr.2024.105112, 2025.

Rohmat, F. I. W., Sa'adi, Z., Stamataki, I., Kuntoro, A. A., Farid, M., and Suwarman, R.: Flood modeling and baseline study in urban and high population environment: A case study of Majalaya, Indonesia, Urban Clim., 46, 101332, https://doi.org/10.1016/j.uclim.2022.101332, 2022.

Ross, C. W., Prihodko, L., Anchang, J. Y., Kumar, S. S., Ji, W., and Hanan, N. P.: Global Hydrologic Soil Groups (HYSOGs250m) for Curve Number-Based Runoff Modeling, ORNL DAAC, Oak Ridge, Tennessee, USA [data set], https://doi.org/10.3334/ORNLDAAC/1566, 2018.

Schubert, J. E., Sanders, B. F., Smith, M. J., and Wright, N. G.: Unstructured mesh generation and landcover-based resistance for hydrodynamic modeling of urban flooding, Adv. Water Resour., 31, 1603–1621, https://doi.org/10.1016/j.advwatres.2008.07.012, 2008.

Sekitar Bandung [sekitarbandungcom]: Jalan Sapan Desa Sumbersari banjir setinggi paha orang dewasa, Instagram, https://www.instagram.com/p/BfhYfIdgf-5/ (last access: 28 July 2026), 23 February 2018.

Shewchuk, J. R.: Triangle: Engineering a 2D quality mesh generator and Delaunay triangulator, in: Applied Computational Geometry: Towards Geometric Engineering, edited by: Lin, M. C. and Manocha, D., Lect. Notes Comput. Sci., 1148, Springer-Verlag, Berlin, Germany, 203–222, 1996.

Soil Conservation Service: Hydrology, in: National Engineering Handbook, Section 4, U.S. Department of Agriculture, Washington, D.C., USA, 1972.

Stability of Solids in Stepped Flume Nappe Flows: Subsidies for Human Stability in Flows, J. Appl. Fluid Mech., 14, https://doi.org/10.47176/jafm.14.03.31815, 2021.

Syuhada, M. M., Oriandra, R. D., Sarifudin, R. A., Wahab, A. A., Farid, M., and Nugroho, J.: Flood Control Study for Cikeruh River Basin in Bandung City, in: Proceedings of the 4th ITB Graduate School Conference, 655–669, 2023.

Laboratoire National d'Hydraulique et Environnement: TELEMAC-2D Software User Manual, Électricité de France (EDF) R&D, Chatou, France, 2023.

USACE Hydrologic Engineering Center: HEC-RAS Hydraulic Reference Manual, Version 6.6, U.S. Army Corps of Engineers, Institute for Water Resources, Davis, California, USA, 2024.

Vu, T., Nguyen, P., Chua, L., and Law, A.: Two-Dimensional Hydrodynamic Modelling of Flood Inundation for a Part of the Mekong River with TELEMAC-2D, Br. J. Environ. Clim. Change, 5, 162–175, https://doi.org/10.9734/BJECC/2015/12885, 2015.

Wang, Z., Chen, Y., Zeng, Z., Chen, X., Li, X., Jiang, X., and Lai, C.: A tight coupling model for urban flood simulation based on SWMM and TELEMAC-2D and the uncertainty analysis, Sustain. Cities Soc., 114, 105794, https://doi.org/10.1016/j.scs.2024.105794, 2024.

Winsemius, H. C., Aerts, J. C. J. H., van Beek, L. P. H., Bierkens, M. F. P., Bouwman, A., Jongman, B., Kwadijk, J. C. J., Ligtvoet, W., Lucas, P. L., van Vuuren, D. P., and Ward, P. J.: Global drivers of future river flood risk, Nat. Clim. Change, 6, 381–385, https://doi.org/10.1038/nclimate2893, 2016.

Wulandari, S., Pratama, F., Andika, N., Wongso, P., Wijayasari, W., and Rohmat, F. I. W.: Identifying dominant river contributions to urban flooding: a scenario-based study of Makassar City, Front. Built Environ., 11, https://doi.org/10.3389/fbuil.2025.1612416, 2025.

Yu, H., Du, L., Lai, C., Luo, P., Wang, Z., and Zeng, Z.: An assessment framework of dam-break flood risk in highly populated and property-intensive area: Case study for the Longdong reservoir, J. Hydrol. Reg. Stud., 58, 102201, https://doi.org/10.1016/j.ejrh.2025.102201, 2025.